Available online at www.sciencedirect.com
ScienceDirect
International Journal of Pharmaceutics 350 (2008) 312–319
INTERNATIONAL JOURNAL OF PHARMACEUTICS
www.elsevier.com/locate/ijpharm

Pharmaceutical Nanotechnology

Tyrosine-derived nanospheres for enhanced topical skin penetration

L. Sheihet [a], P. Chandra [a], P. Batheja [b], D. Devore [a], J. Kohn [a], B. Michniak [a,b,*]

[a] *New Jersey Center for Biomaterials, Rutgers – The State University of New Jersey, 145 Bevier Road, Piscataway, NJ 08854, United States*
[b] *Ernest Mario School of Pharmacy, Rutgers – The State University of New Jersey, 160 Frelinghuysen Road, Piscataway, NJ 08854, United States*

Received 25 May 2007; received in revised form 14 August 2007; accepted 15 August 2007
Available online 23 August 2007

Abstract

The objective of this study was to investigate the passive skin penetration of lipophilic model agents encapsulated within tyrosine-derived nanospheres. The nanospheres were formed by the self-assembly of a biodegradable, non-cytotoxic ABA triblock copolymer. The A-blocks were poly(ethylene glycol) and the hydrophobic B-blocks were oligomers of suberic acid and desaminotyrosyl-tyrosine alkyl esters. These nanospheres had an average hydrodynamic diameter of about 50 nm and formed strong complexes with fluorescent dyes, 5-dodecanoylaminofluorescein (DAF, Log D = 7.54) and Nile Red (NR, Log D = 3.10). These dyes have been used here as models for lipophilic drugs. The distribution of topically applied nanosphere-dye formulations was studied in human cadaver skin using cryosectioning and fluorescence microscopy. Permeation analysis (quantified fluorescence) over a 24 h period revealed that the nanospheres delivered nine times more NR to the lower dermis than a control formulation using propylene glycol. For DAF, the nanosphere formulation was 2.5 times more effective than the propylene glycol based control formulation. We conclude that tyrosine-derived nanospheres facilitate the transport of lipophilic substances to deeper layers of the skin, and hence may be useful in topical delivery applications.

Keywords: Biodegradable nanospheres; Topical delivery; Skin penetration; Lipophilic; Fluorescence

1. Introduction

Skin penetration enhancement is needed because intact skin is not sufficiently permeable to most drugs. Numerous physical and chemical enhancement approaches have been investigated and can be divided into active or passive methods. Active methods provide an extra driving force for drug permeation and include techniques such as iontophoresis (electrical gradient), electroporation (short high voltages), use of microneedles (mechanical approach), ultrasound, laser and photomechanical waves (Brown et al., 2006). Passive methods include the use of penetration enhancers (Williams and Barry, 2004), supersaturated systems (Pellet et al., 2003), prodrug or metabolic approaches (Elias et al., 2003), liposomes, microemulsions, and colloidal polymeric suspensions (Cevc, 2004; El Maghraby et al., 2006; Godin and Touitou, 2003; Vila et al., 2002) to increase the rate of drug diffusion and/or increase the permeability of skin.

To date, the above enhancement methods have had only limited impact as the amount of drug that can be delivered is still limited and only small, moderately lipophilic and potent drugs can be considered for percutaneous or transdermal administration. Also, a common side effect of penetration enhancers is that the barrier function of the stratum corneum is disturbed for long periods of time after skin application (Man et al., 1993), resulting in a more sensitive skin and irritancy.

Recently, we reported on an extended family of amphiphilic ABA-triblock copolymers that consist of hydrophilic A-blocks of poly(ethylene glycol) and hydrophobic B-blocks of desaminotyrosyl-tyrosine alkyl esters (DTR) and diacids (Nardin et al., 2004; Sheihet et al., 2005). These copolymers self-assemble in aqueous solution to form nanospheres

Abbreviations: DTO, desaminotyrosyl-tyrosine octyl ester; SA, suberic acid; PEG, poly(ethylene glycol); NSP, nanosphere(s); PG, propylene glycol; DAF, 5-docecanoylaminofluorescein; NR, Nile Red; NSP-DAF and NSP-NR, nanosphere-5-docecanoylaminofluorescein and nanosphere-Nile Red formulations; PG-DAF and PG-NR, propylene glycol-5-docecanoylaminofluorescein and propylene glycol-Nile Red solution; SD, superficial dermis; LD, lower dermis; PE, penetration effect (analysis of fluorescent intensity recorded in skin sections); S.E., standard error

* Corresponding author at: New Jersey Center for Biomaterials, Rutgers – The State University of New Jersey, 145 Bevier Road, Piscataway, NJ 08854, United States. Tel.: +1 732 445 3589; fax: +1 732 445 5006.
E-mail address: michniak@biology.rutgers.edu (B. Michniak).

0378-5173/$ – see front matter © 2007 Elsevier B.V. All rights reserved.
doi:10.1016/j.ijpharm.2007.08.022

with hydrodynamic diameters between 40 and 70 nm, that do not dissociate under chromatographic and ultracentrifugation conditions. Previous studies established the lack of cellular toxicity of these nanospheres, as well as their tendency to form strong complexes with paclitaxel, a widely used hydrophobic chemotherapeutic agent (Sheihet et al., 2005; Sheihet et al., 2007b). Further, no acute toxicity, skin irritation or sensitization was detected when mice were injected with nanospheres, and the anti-tumor efficacy of nanospheres-paclitaxel was confirmed in mice bearing subcutaneous breast cancer xenografts (Sheihet et al., 2007a).

Since so far only a limited number of biodegradable, polymer microparticles (Berthold et al., 1998; De Jalon et al., 2001; Santoyo et al., 2002) and solid-lipid nanoparticles (Borgia et al., 2005; Chen et al., 2006; Muller et al., 2002) have been investigated as skin penetration enhancers, we extended the application of these tyrosine-derived nanospheres to delivery vehicles for highly lipophilic molecules for passive skin permeation. Fluorescent dyes, DAF and Nile Red, were used as model compounds to determine the efficiency of the nanosphere approach as compared to commonly used propylene glycol-based control formulations (Bendas et al., 1995).

2. Materials and methods

2.1. Materials

Methylene chloride (HPLC grade), methanol (HPLC grade), 2-propanol and optimal cutting temperature compound (OCT) were purchased from Fisher Scientific, (Pittsburgh, PA). Suberic acid, 4-dimethylaminopyridinium-*p*-toluene sulfate (DMPTS), propylene glycol (PG), poly(ethylene glycol) monomethyl ether (Mw 5000) and Dulbecco's phosphate buffered saline (PBS, pH 7.4) were purchased from Aldrich Chemical Co. (Milwaukee, WI). Diisopropylcarbodiimide (DIPC) was purchased from Tanabe Chemicals (San Diego, CA). *N,N*-dimethylformamide (DMF) and tetrahydrofuran (THF) were obtained from Merck (EM Science, Darmstadt, Germany), and dimethyl sulfoxide (DMSO) was obtained from Merck and Sigma. 5-Dodecanoylaminofluorescein (DAF) and Nile Red (NR) were obtained from Molecular Probes (Eugene, OR). All reagents were used as received.

2.2. Methods

2.2.1. Polymer preparation and characterization

The triblock copolymer was synthesized in a one-pot reaction at 20 °C using *in situ* carbodiimide coupling of the poly(ethylene glycol) monomethyl ether, PEG, and oligo(DTO-SA) as described before (Nardin et al., 2004; Sheihet et al., 2005). The chemical structure and purity of the copolymer were confirmed by ^{1}H NMR (d_6-DMSO, Varian Unity 300 spectrophotometer, Palo Alto, CA). Molecular weights (Mn and Mw) were determined using gel permeation chromatography, GPC (PL-gel columns, pore size 10^5 and 10^4 Å, Perkin-Elmer, Shelton, CT; Waters 410 RI detector) with 1 mL/min THF flow rate and polystyrene standards as Mw markers.

2.2.2. Preparation of nanosphere-model compounds formulations

Nanosphere complexes with or without model compounds were prepared by combining 60 mg of triblock copolymer with 600 μg of either DAF or NR in 600 μL of DMF. These solutions were added drop-wise to 14.4 mL of deionized water with constant stirring to produce turbid aqueous dispersions. *We refer to purified nanospheres as those that were processed as follows*: the self-assembled nanosphere-solute suspensions were filtered through 0.22 μm PVDF syringe filters (Millipore, Bedford, MA) in order to remove particles greater than 220 nm in diameter. Next, purified nanospheres were isolated by ultracentrifugation of 12.25 mL of filtered nanosphere solutions at 65 000 rpm (290 000 × *g*) for 3 h at 25 °C (Beckman L8-70M ultracentrifuge, Beckman Coulter, Fullerton, CA). Following the removal of the supernatant, the pelleted nanospheres were washed twice with PBS, and re-suspended with gentle agitation in 1 mL of PBS at 25 °C. Then, the volume of the re-suspended pellets was increased to 3 mL by the addition of PBS, and finally, the solutions were again filter-sterilized (0.22 μm). Purified nanospheres alone and nanosphere-model compound formulations were used for all subsequent characterizations.

2.2.3. Characterization of nanosphere-model compound formulations

2.2.3.1. Size, size distribution and morphology. The hydrodynamic diameter of the nanospheres was obtained using dynamic light scattering at $q = 90^\circ$, $\lambda = 523$ nm and $T = 298$ K using cumulant fit analysis (Lexel argon ion laser, Fremont, CA; Brookhaven Instruments goniometer and correlator BI-2030; Holtsville, NY).

The morphology of nanospheres was determined using transmission electron microscopy (TEM). For the negative staining experiments, a drop of the nanosphere dispersion was allowed to settle on a Formvar pre-coated grid for 1 min. The excess sample was removed by gentle blotting with filter paper and a drop of staining solution (2% uranyl acetate) was allowed to contact the sample for 1 min. Then, the excess stain was removed carefully by touching the grid edge by the edge of a filter paper wedge (Harris et al., 1999). For the Pt/C shadow method experiments, a drop of nanospheres was applied onto a copper Formvar/Carbon coated grid for ~1 min. Excess fluid was removed by gently blotting the grid with the edge of a torn piece of filter paper. The grids were air-dried and shadowed with 2.5 nm Pt/C (30°) using High Vacuum Freeze-Etch unit BAF 300 (Balzers, Elgin, IL) (Ruben, 1995). Electron micrographs were taken on a model JEM 100CX Transmission Electron Microscope (JEOL LTD, Peabody, MA).

2.2.3.2. Model compound (dye) binding efficiency. Sensitive, specific and reproducible high-performance liquid chromatography (HPLC) methods were developed and validated for quantitative determination of Nile Red and DAF in the copolymer system. Dye concentration was assayed using a Waters 2695 HPLC system equipped with UV–vis detector (Waters 2487, Dual 1 Absorbance Detector) and a RP-C18 column (Perkin-Elmer Brownlee Analytical C-18 column, 33 mm × 4.6 mm)

following a previously described protocol (Sheihet et al., 2007b). The mobile phase was a mixture of water (0.1% TFA)/acetonitrile (0.1% TFA) with the ratio of 35/65 (v/v) and 40/60 (v/v) for the assay of DAF and NR, respectively. The UV–vis detector was set at 550 and 270 nm for NR and DAF, respectively. The detection limits were evaluated on the basis of a signal to noise ratio of 3 and were 0.04 μg/mL for NR and 0.07 μg/mL for DAF. Intra- and inter-day precision and accuracy determination of quality control samples were better than 10% across the range of the calibration curve.

To determine the dye binding efficiency, a predetermined aliquot of the purified nanosphere-dye complex suspension was withdrawn and freeze-dried. Then, the dry residue was accurately weighed before thoroughly dissolving for 1 h in the extraction solvent: 5 mL of EtOH and 5 mL of MeOH for Nile Red and DAF respectively. Model agents' complexation by the nanospheres was characterized by the following ratio:

$$\text{Binding efficiency (\%)} = \frac{\text{mass of dye in the nanospheres}}{\text{mass of initial dye used}}$$

Solutions of each dye in propylene glycol (PG) were prepared by stirring an excess of the molecule in PG at room temperature for 24 h. The samples were filtered through 0.22 μm PVDF syringe filters (Millipore, Bedford, MA), and the filtrates were used for all subsequent characterizations and experiments. For passive permeation experiments, the equivalent concentration (confirmed using RP-HPLC) of all dyes in both propylene glycol and nanospheres was achieved by subsequent dilution of either PG-dye solution with PG or NSP-dye formulation with PBS.

2.2.4. Skin permeation tests

2.2.4.1. Human skin. The full thickness dermatomed (~500 μm) human skin derived from the abdominal regions of female Caucasian cadavers were obtained from AlloSource (Englewood, CO) and stored at −80 °C. Just before each experiment, the skin was allowed to thaw to room temperature and then used immediately for *in vitro* transport studies.

2.2.4.2. Transport studies. Pieces of full thickness human skin were mounted on Franz diffusion cells (PermeGear, Bethlehem, PA) and hydrated as described previously (Meidan et al., 2003). Next, 0.3 mL of the appropriate formulation of each dye (in NSP or PG) was deposited on to the surface of skin samples for 24 h and 1, 3, 6 h in case of NR time-dependency permeation experiments. The skin of the same donor was used for verum and control experiments for each dye. Time-dependency and 24-h permeation studies were performed using skin from different donors. In all experiments, the donor compartment of the sampling port of each Franz cell was covered with a taught layer of Parafilm®, and the whole set up was roofed with aluminum foil to prevent the bleaching of the dye. Each permeation experiment was conducted in sextuplicate or quadruplicate (in case of time-dependency experiments). At the end of the permeation experiment, the excess formulation was removed from the skin surface, skin sections were detached from the diffusion cells, washed three times with PBS, and dried gently with delicate task wipes (Kimwipes). The skin pieces were frozen at −20 °C, 0.2 cm × 0.5 cm piece from the treated area was cut out and embedded in optimal cutting temperature compound (OCT). A cryostat (Leica Cryostat CM 3050S, Wetzlar, Germany) was used to prepare the vertical cross-sections of skin. Nine to twelve vertical sections of each sample with a thickness of 20 μm were obtained and stored at 4 °C till analyzed microscopically.

2.2.4.3. Fluorescent microscopy. Skin sections were subjected to both fluorescent and phase-contrast microscopy using Olympus CK40 microscope equipped with a UV source and filters for fluorescent measurement. Image capture and analysis were carried out using Olympus Microsuite TM B35V program. The excitation and emission wavelengths were for 485 and 520 nm for DAF and 546 and 585 nm for Nile Red, respectively. Images were recorded setting the camera integration time of 500 ms. The same parameters were used for imaging all samples and no correction for the background fluorescence was made. Fluorescence yield was quantified using the image treatment software (ImageJ, v1.36, NIH); the integration of pixel brightness values (arbitrary units, ABU) gives the relative dye content.

2.2.4.4. Histology of cryosectioned skin using hematoxylin and eosin staining. Histology of the skin sections obtained by cryosectioning was examined using the modification of hematoxylin and eosin (H&E) staining procedure provided by the manufacturer. Briefly, skin sections were hydrated in distilled water for 1 min and then stained with Gill 2 Hematoxylin (Sigma, St. Louis, MO) for 4 min. Excess stain was washed off by rinsing the slides in distilled water three times, for 1 min each, followed by the addition of Scott's solution (0.1% sodium bicarbonate) for 2 min. After a brief rinse in distilled water the skin sections were counter-stained in acidified Eosin Y (Sigma, St. Louis, MO) for 3 min. Slides were sequentially dehydrated using 95% ethanol, followed by 80% and 70% ethanol (1 min each). After clearing in three changes of xylene for 1 min each, the slides containing skin sections were mounted using a Paramount mounting medium, dried overnight and analyzed microscopically.

2.3. Data analysis

The images presented in Figs. 3–5 are representative and attempt to capture what was typically observed under control and treatment conditions. To assure appropriate representation, each image selected was an average of 30–40 replicates of skin sections. The statistical data were analyzed using Student's *t*-test and expressed as the mean value ± S.E. (standard error); $p < 0.01$ (*) was considered to be statistically significant.

3. Results and discussion

3.1. Nanospheres characterization: design, size and morphology

The general chemical structure of the tyrosine-based triblock copolymer is illustrated in Scheme 1. The hydrophobic middle block was prepared by reacting DTO with suberic acid resulting

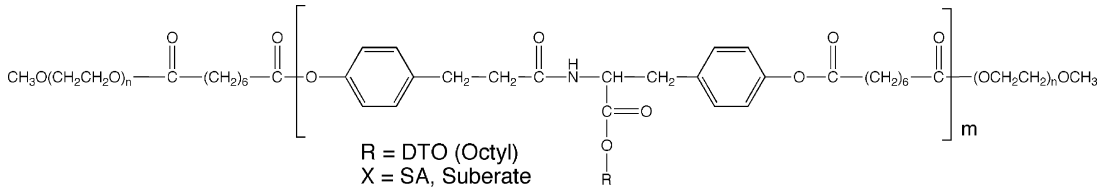

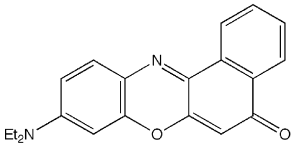

Nile Red (Log D 3.10)

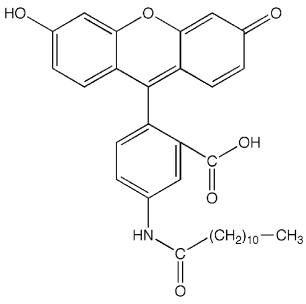

DAF (Log D 7.54)

Scheme 1. Structures of PEG-*b*-oligo(DTO-SA)-*b*-PEG triblock copolymer, 5-dodecanoylaminofluorescein (DAF) and Nile Red. Log D values (pH 7) were obtained from ACD/Labs (© 1994–2006 ACD/Labs).

in oligomers with carboxylic acid end groups that were further reacted with PEG using a previously published procedure (Nardin et al., 2004; Sheihet et al., 2005).

The design of this copolymer system was based on the following rational: PEG end blocks are well characterized and known to be non-cytotoxic and biocompatible (Greenwald et al., 2003); the modulation of cell behavior and non-fouling characteristics of PEG makes it attractive for *in vivo* applications (Vila et al., 2002). The choice of the oligo(DTO suberate) for the middle block was based on its low glass transition temperature Tg (294 K), which ensures that each triblock copolymer molecule will be sufficiently flexible to self-assemble into a dynamic and non-frozen structure (Nardin et al., 2004). In addition, this middle block is degradable under physiological conditions (Bourke and Kohn, 2003). The spherical morphology and nano-scale dimension of the nanospheres were demonstrated by electron microscopy and dynamic light scattering measurements. The size distributions of nanosphere-dye complexes are shown in Fig. 1. The average hydrodynamic diameter

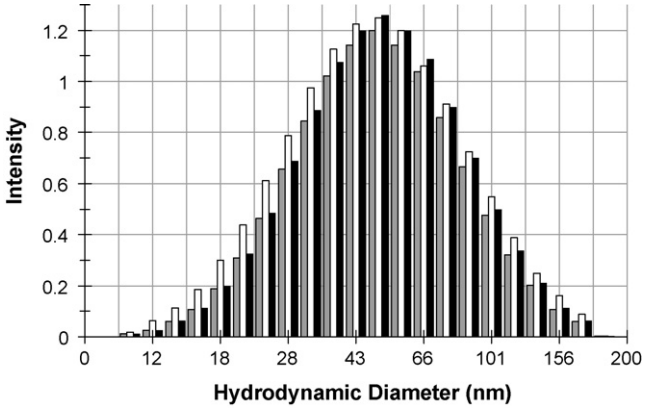

Fig. 1. The size distribution of solute-nanosphere formulations as measured by dynamic light scattering (Cumulant fit). (Black) nanosphere-Nile Red; (Empty) nanosphere-DAF complexes; (Grey) nanosphere alone.

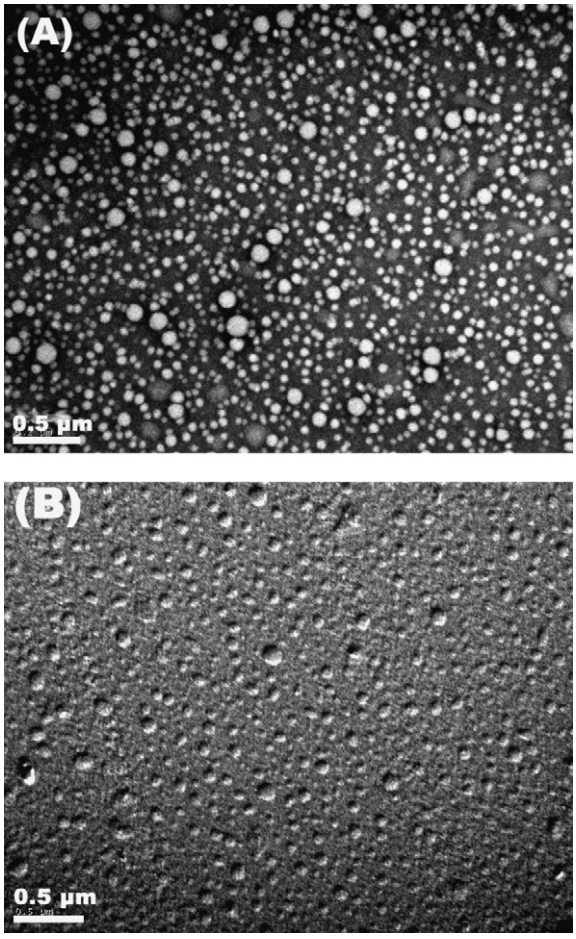

Fig. 2. Transmission electron microscopy (TEM) images of nanospheres made of PEG-*b*-oligo(DTO-SA)-*b*-PEG triblock copolymer in aqueous solution. (A): negative staining method (2% uranyl acetate); (B): Pt/C shadow method.

of the nanospheres prepared in the absence or presence of different model compounds had a relatively narrow size distribution centered around 55 nm, indicating that neither the presence of dye in the nanosphere preparation nor its hydrophobicity had a significant effect on nanosphere size. Fig. 2 illustrates the spherical morphology of the nanospheres obtained by transmission electron microscopy. However, their size distribution appears to be larger than observed by light scattering analysis, ranging from 30 to 200 nm in diameter. This difference is most probably an artifact, due to drying of the specimens prior to electron microscopy (leading to shrinkage and/or agglomeration of the nanospheres). Assuming that the average width of transepidermal hydrophilic pathways is in order of 0.4 nm (water evaporation pathways) to up to about 100 nm (intercorneocyte space) (Cevc, 2004), the relatively small size of tyrosine-derived nanospheres will easily allow their penetration into the stratum corneum along the surface furrows on the skin.

3.2. Nanosphere-dye formulations

The fluorophores of choice, DAF and NR (Scheme 1), have been used previously for visualizing of micelles and liposomes within cells and skin (Alvarez-Roman et al., 2004; Savic et al., 2004). A binding efficiency of 65% was obtained for both model dyes regardless of the extent of their hydrophobicity and molecular weight. The dye-binding efficiency was measured following filtration through 0.22 μm filters, ultracentrifugation and a second filtration through 0.22 μm filters under sterile conditions. The initial filtration step strongly affected the measured binding efficiency because all nanospheres larger then 220 nm were removed. The concentration of model dyes in the final nanosphere preparations used for all subsequent studies was 180 μg/mL for DAF and 200 μg/mL for NR; hence the nanosphere-dye formulations were compared against 0.02% PG-dye solutions in all skin permeation studies. These formulations provided a sufficiently strong signal to be detected by fluorescent microscopy.

3.3. Cutaneous uptake

In order to explore the potential of tyrosine-derived nanospheres for topical delivery, the permeation ability of NSP-model agent complexes into human cadaver skin was evaluated *in vitro* using Franz diffusion cells. Passive permeation involving 24 h topical application of dye in NSP and PG to human cadaver skin revealed that the amount of dyes in the receptor compartments, if any, was below the limit of detection by HPLC analysis. This result confirmed that nanospheres do not facilitate transdermal penetration across human cadaver skin. This is in agreement with previously reported observations that the use of particulate drug carriers appeared to improve the drug residence in skin without increasing transdermal transport (Alvarez-Roman et al., 2004).

Images of skin treated with PBS and/or nanospheres alone did not reveal any fluorescent signal, and hence contribution of skin and/or nanospheres auto-fluorescence to the total fluorescence detected was negligible. Fig. 3 depicts representative examples of fluorescence microscopy images of vertically cross-sectioned skin following topical application of DAF and Nile Red for 24 h. Qualitatively, nanospheres clearly promoted penetration of dyes into deeper layers of skin as compared to propylene glycol (Fig. 3, A versus B and C versus D). Quantitative analysis of dye penetration was obtained from pixel intensities derived from

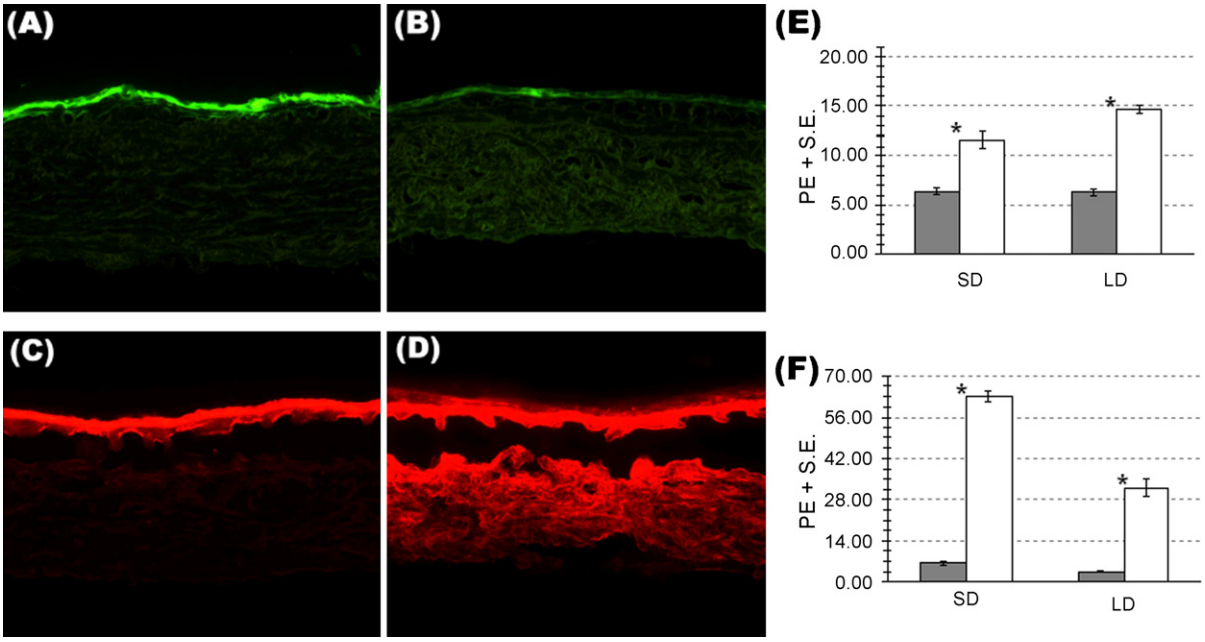

Fig. 3. Cross-sectional fluorescent images obtained following 24 h of passive permeation. (A) PG-DAF; (B) NSP-DAF; (C) PG-NR; (D) NSP-NR. Penetration effect (PE ± standard error, $^{*}p < 0.01$) of NSP with respect to PG after 24 h of passive permeation. (Grey box) PG and (empty box) NSP: (E) DAF; (F) NR. SD: superficial dermis; LD: lower dermis.

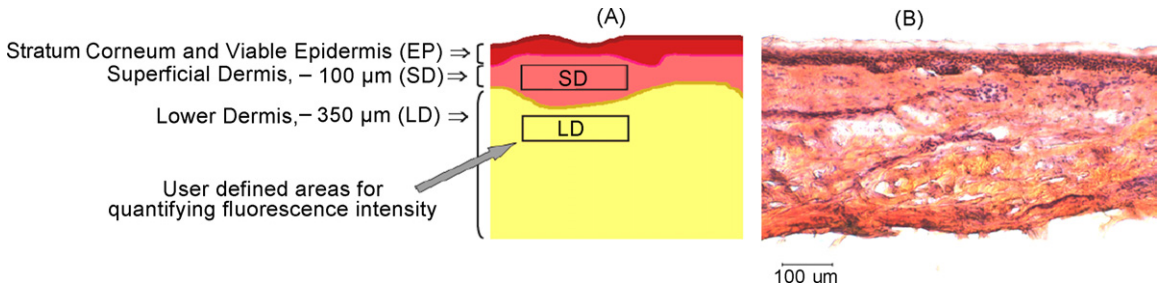

Fig. 4. Schematic representation of cryosectioned skin (A) and H&E staining (B).

fluorescence measurements of the skin sections. Image analysis was carried out for the superficial dermis (SD) and lower dermis (LD) as schematically represented in Fig. 4(A). In this study, the superficial dermis is defined as the region measuring around 100 μm below the viable epidermis and the lower dermis is the remaining portion of the skin below the superficial dermis. H&E staining of skin section (Fig. 4B) was used to define the above layers. The fluorescence intensities of DAF and NR in different layers of skin are expressed in arbitrary units (ABU) and are shown in Fig. 3(E and F). The 24 h studies showed that the dye penetration was much greater using nanospheres as compared to propylene glycol (Fig. 3B and D). The fluorescence intensity in the superficial dermis of skin samples (Fig. 3E and F, $p < 0.01$) treated with nanosphere-DAF complexes was 2 times higher than for propylene glycol-DAF formulations. Nanosphere-NR complexes produced 10 times higher fluorescence than propylene glycol-NR formulations. Similarly in the lower dermis, the distribution of dyes delivered via nanospheres resulted in about 2.5-fold and 9-fold increase ($p < 0.01$) for DAF and NR, respectively (Fig. 3E and F). Similar observations were reported by Alvarez-Roman et al., showing enhanced NR penetration for a particulate vehicle as compared to PG-NR solutions (Alvarez-Roman et al., 2004).

In this study, NSP-dyes and PG-dyes penetration to epidermis (stratum corneum and viable epidermis) was not quantified or compared. It has been reported that propylene glycol contributes to increased stratum corneum localization, but decreased permeability and solute diffusion into the deeper skin (Hatanakaa et al., 1993; Walker and Smith, 1996). Therefore, the intense fluorescence observed in epidermis strata could be attributed to the viscous nature of PG, in contrast to an aqueous solution of nanospheres (Fig. 3A and C). Nonetheless, in this study the choice of PG as a control was mainly based on its ability to solubilize DAF and NR, its non-particulate and neutral nature, and previous use as a control in similar studies (Alvarez-Roman et al., 2004; Pillai et al., 2004).

Penetration kinetics of Nile Red delivered via nanospheres and propylene glycol are represented in Fig. 5. A significant difference ($p < 0.01$) in the fluorescence intensity was detected in all skin layers after 1 h of exposure to nanosphere-NR complexes, as compared to PG-NR (Fig. 5A-1 and B-1). The measured PE values in the superficial dermis were 6.5 ± 0.2 and 9.5 ± 0.3 for PG-NR and NSP-NR, respectively. In the lower dermis these values were 7.6 ± 0.4 for control sample (PG) and 13.6 ± 1.2 for NSP-NR. This suggests that dye penetration into lower dermis is much faster and about 45% higher when applied in nanosphere formulation (Fig. 5, LD).

No considerable enhancement fluorescence intensity of NR was observed between 1 and 3 h of PG-NR application (Fig. 5A-3 versus A-1). In contrast, with NSP-NR, about 42% increase in intensity was observed from 1 to 3 h (Fig. 5 SD and LD). The 6 h treatment further increased Nile Red penetration via both vehicles, but the enhancement due to NSP was about 45% higher as compared to PG (Fig. 5A-6 and B-6 and corresponding charts). In addition, 3 and 6 h of NSP-NR application showed a significantly higher dye accumulation in SD, but not in LD strata (Figs. 5 and 3-F). This suggests the potential of these nanospheres in controlled delivery of drugs to the sites of disorders located within the dermoepidermal junction and the superficial dermis.

The greater extent of skin penetration of nanosphere-dye formulations could be most likely attributed to: (1) vehicle nature, (2) size and (3) mechanism of penetration. First, although both nanospheres and propylene glycol are good solvents for DAF and NR, the application of neat PG may also have a dehydrating effect on the skin thereby contributing to less flux (Ward and Osborne, 1993). In contrast, the presence of PEG in the nanosphere corona could provide superior hydration of the skin, therefore exhibiting a permeation enhancing effect (Gupta and Jain, 2004). An individual nanosphere could be considered as a supersaturated system, that is, the maximum quantity of dye that was encapsulated during the preparation. The same concentration of dye in propylene glycol was below the saturation limit. Hence, the superior thermodynamic activity of the dye in the nanosphere is expected to increase the partitioning (Alvarez-Roman et al., 2004). Second, nano-sized vehicles are advantageous to improve skin penetration and also drug accumulation, as was demonstrated for solid lipid nanoparticles (Cevc, 2004; Liu et al., 2007). Given the small size, size distribution and dynamic structure of nanosphere-dye complexes, it is conceivable that they may traverse through the intercorneocyte spaces (Barry, 2001). Third, an increase in penetration extent may result from an alteration in the barrier properties and/or a greater degree of partitioning of the nanospheres into the stratum corneum (Barry, 2004). It is possible that the furrows between the corneocyte islands provide a place into which nanospheres may accumulate within the skin. In future studies, mechanism of nanospheres penetration, cellular uptake, potential toxicity in skin cells and topical delivery of lipophilic drugs will be investigated.

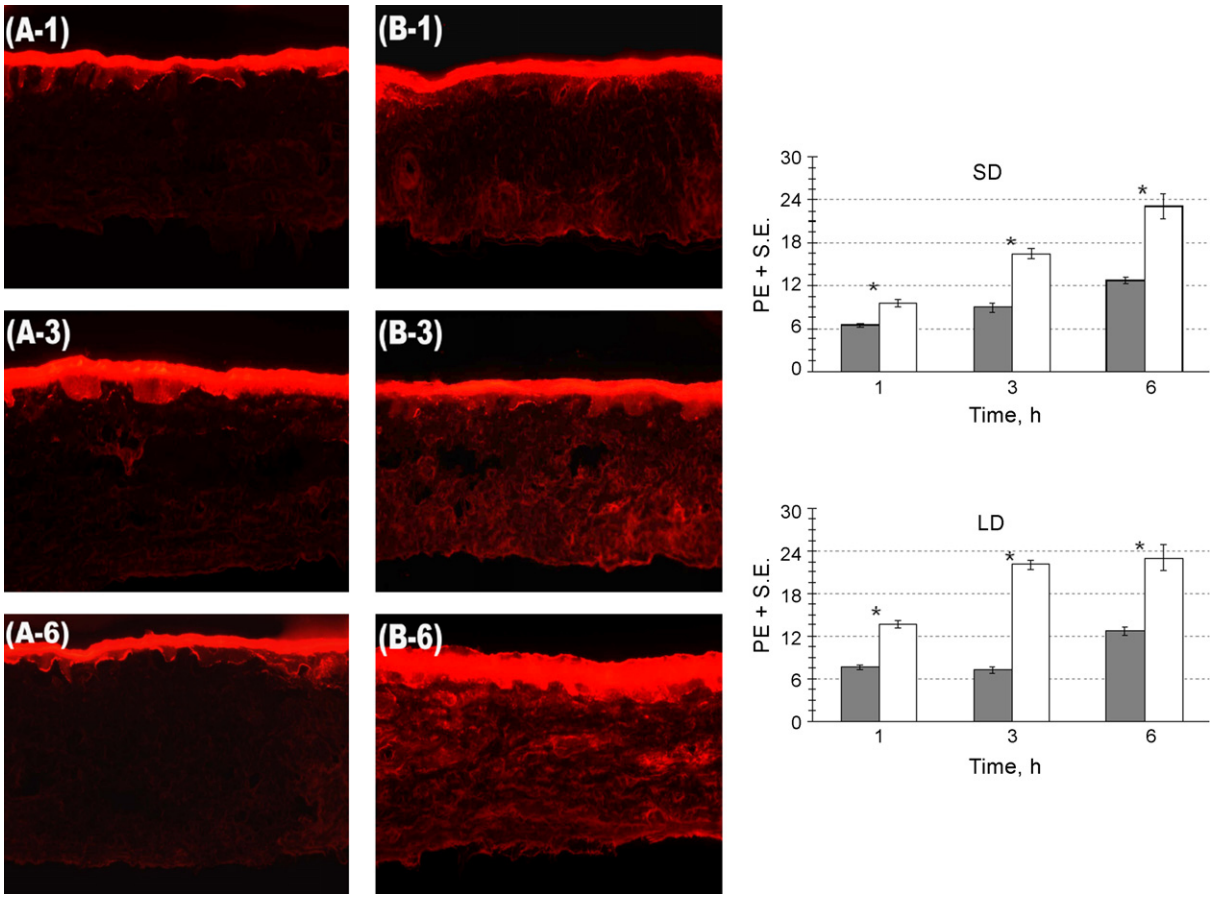

Fig. 5. Cross-sectional images obtained following 1, 3 and 6 h of passive permeation. (A-time) PG-NR; (B-time) NSP-NR. Penetration effect (PE ± standard error, $^{*}p < 0.01$) of NSP with respect to PG after 1, 3, and 6 h of passive permeation. (Grey box) PG-NR and (empty box) NSP-NR: SD: superficial dermis; LD: lower dermis.

4. Conclusions

Tyrosine-derived nanospheres significantly enhanced skin penetration of highly lipophilic model compounds (DAF and Nile Red) in human cadaver skin as compared to a non-particulate formulation at the same concentration. No detectable transdermal permeation was observed even after 24 h application, suggesting that these nanospheres can be used in topical drug delivery. An increase in rate and extent of dyes penetration to deeper skin layers could be due to the higher thermodynamic activity of the dye (relative to that in propylene glycol), small size and hydration properties of the nanospheres. Tyrosine-derived nanospheres have previously shown highly effective delivery of hydrophobic anti-tumor drugs to human tumor cells *in vitro* without the cytotoxicity effects exhibited by surfactant-based excipients (Sheihet et al., 2007a,b). Hence, these nanospheres can offer a promising tool for the topical skin delivery of lipophilic drugs and personal care agents such as Vitamins A and D, sunscreens, glucocorticoids, or retinoids.

Acknowledgments

The authors thank Dr. Gleb Shumyatsky for use of the cryostat. Support for this work from the New Jersey Center for Biomaterials and CEMBR grant W81XWH-04-2-003 are acknowledged.

References

Alvarez-Roman, R., Naik, A., Kalia, Y.N., Guy, R.H., Fessi, H., 2004. Enhancement of topical delivery from biodegradable nanoparticles. Pharm. Res. 21, 1818–1825.

Barry, B.W., 2001. Novel mechanisms and devices to enable successful transdermal drug delivery. Eur. J. Pharm. Sci. 14, 101–114.

Barry, B.W., 2004. Breaching the skin's barrier to drugs. Nat. Biotechnol. 22, 192–197.

Bendas, B., Schmalfuβ, U., Neubert, R., 1995. Influence of propylene glycol as cosolvent on mechanisms of drug transport from hydrogels. Int. J. Pharm. 116, 19–30.

Berthold, A., Cremer, K., Kreuter, J., 1998. Collagen microparticles: carriers for glucocorticosteroids. Eur. J. Pharm. Biopharm. 45, 23–29.

Borgia, S.L., Regehly, M., Sivaramakrishnan, R., Mehnert, W., Korting, H.C., Danker, K., Roder, B., Kramer, K.D., Schafer-Korting, M., 2005. Lipid nanoparticles for skin penetration enhancement-correlation to drug localization within the particle matrix as determined by fluorescence and parelectric spectroscopy. J. Controlled Release 110, 151–163.

Bourke, S.L., Kohn, J., 2003. Polymers derived from the amino acid L-tyrosine: polycarbonates, polyarylates and copolymers with poly(ethylene glycol). Adv. Drug Del. Rev. 55, 447–466.

Brown, M.B., Martin, G.P., Jones, S.A., Akomeah, F.K., 2006. Dermal and transdermal drug delivery systems: current and future prospects. Drug Deliv. 13, 175–187.

Cevc, G., 2004. Lipid vesicles and other colloids as drug carriers on the skin. Adv. Drug Deliv. Rev. 56, 675–711.

Chen, H., Chang, X., Du, D., Liu, W., Liu, J., Weng, T., Yang, Y., Xu, H., Yang, X., 2006. Podophyllotoxin-loaded solid lipid nanoparticles for epidermal targeting. J. Controlled Release 110, 296–306.

De Jalon, E.G., Blanco-Prieto, M.J., Ygartua, P., Santoyo, S., 2001. PLGA microparticles: possible vehicles for topical drug delivery. Int. J. Pharm. 226, 181–184.

El Maghraby, G.M., Williams, A.C., Barry, B.W., 2006. Can drug-bearing liposomes penetrate intact skin? J. Pharm. Pharmacol. 58, 415–429.

Elias, P.M., Feingold, K.R., Tsai, J., 2003. Metabolic approach to transdermal drug delivery. In: Guy, R.H., Hadgraft, J. (Eds.), Transdermal drug delivery, second ed. Marcel Dekker, New York.

Godin, B., Touitou, E., 2003. Ethosomes: new prospects in transdermal delivery. Crit. Rev. Ther. Drug Carrier Syst. 20, 63–102.

Greenwald, R.B., Choe, Y.H., Mcguire, J., Conover, C.D., 2003. Effective drug delivery by PEGylated drug conjugates. Adv. Drug Deliv. Rev. 55, 217–250.

Gupta, S.P., Jain, S.K., 2004. Development of matrix-membrane transdermal drug delivery system for atenolol. Drug Deliv. 11, 281–286.

Harris, J.R., Roos, C., Djalali, R., Rheingans, O., Maskos, M., Schmidt, M., 1999. Application of the negative staining technique to both aqueous and organic solvent solutions of polymer particles. Micron 30, 289–298.

Hatanakaa, T., Shimoyamaa, M., Sugibayashia, K., Morimotoa, Y., 1993. Effect of vehicle on the skin permeability of drugs: polyethylene glycol 400-water and ethanol–water binary solvents. J. Controlled Release 23, 247–260.

Liu, J., Hu, W., Chen, H., Ni, Q., Xu, H., Yang, X., 2007. Isotretinoin-loaded solid lipid nanoparticles with skin targeting for topical delivery. Int. J. Pharm. 328, 191–195.

Man, M.Q., Feingold, K.R., Elias, P.M., 1993. Exogenous lipids influence permeability barrier recovery in acetone-treated murine skin. Arch. Dermatol. 129, 728–738.

Meidan, V.M., Al-Khalili, M., Michniak, B.B., 2003. Enhanced iontophoretic delivery of buspirone hydrochloride across human skin using chemical enhancers. Int. J. Pharm. 264, 73–83.

Muller, R.H., Radtke, M., Wissing, S.A., 2002. Solid lipid nanoparticles (SLN) and nanostructured lipid carriers (NLC) in cosmetic and dermatological preparations. Adv. Drug Deliv. Rev. 54, S131–S155.

Nardin, C., Bolikal, D., Kohn, J., 2004. Nontoxic block copolymer nanospheres: design and characterization. Langmuir 20, 11721–11725.

Pellet, M., Raghavan, S.L., Hadgraft, J., Davis, A.F., 2003. The application of supersaturated systems to percutaneous drug delivery. In: Guy, R.H., Hadgraft, J. (Eds.), Transdermal drug delivery, second ed. Marcel Dekker, New York.

Pillai, O., Kumar, N., Dey, C.S., Borkute, Sivaprasad, N., Panchagnula, R., 2004. Transdermal iontophoresis of insulin: III. Influence of electronic parameters. Methods Find Exp. Clin. Pharmacol. 26, 399–408.

Ruben, G.C., 1995. Quantification of particle sizes with metal replication under standard freeze-etching conditions: a gold ball standard for calibrating shadow widths was used to measure freeze-etch globular proteins. Microsc. Res. Tech. 32, 312–329.

Santoyo, S., Ga De Jalon, E., Ygartua, P., Renedo, M.J., Blanco-Prieto, M.J., 2002. Optimization of topical cidofovir penetration using microparticles. Int. J. Pharm. 242, 107–113.

Savic, R., Luo, L., Eisenberg, A., Maysinger, D., 2004. Micellar nanocontainers distribute to defined cytoplasmic organelles. Science 303, 626–628.

Sheihet, L., Dubin, R.A., Devore, D., Kohn, J., 2005. Hydrophobic drug delivery by self-assembling triblock copolymer-derived nanospheres. Biomacromolecules 6, 2726–2731.

Sheihet, L., Kohn, J., Devore, D., Rubin, E.H., Gounder, M.K., 2007a. Development of a Novel Biodegradable Nanospheres-Paclitaxel Formulation as a Potential Anti-Cancer Agent: Evaluation of Toxicity and Efficacy in Comparison with Cremophor-Based Paclitaxel. The Annual Retreat on Cancer Research in New Jersey, New Jersey.

Sheihet, L., Piotrowska, K., Dubin, R.A., Kohn, J., Devore, D., 2007b. Effect of tyrosine-derived triblock copolymer compositions on nanosphere self-assembly and drug delivery. Biomacromolecules 8, 998–1003.

Vila, A., Sanchez, A., Perez, C., Alonso, M.J., 2002. PLA-PEG nanospheres: new carriers for transmucosal delivery of proteins and plasmid DNA. Polym. Adv. Technol. 13, 851–858.

Walker, R.B., Smith, E.W., 1996. The role of percutaneous penetration enhancers. Adv. Drug Deliv. Rev. 18, 295–301.

Ward, A.J.P., Osborne, D.W., 1993. Hydrotropy and Penetration Enhancement. Pharmaceutical Skin Penetration Enhancement. Marcel Dekker Inc., New York.

Williams, A.C., Barry, B.W., 2004. Penetration enhancers. Adv. Drug Deliv. Rev. 56, 603–618.